Proceedings of the 28th IEEE
EMBS Annual International Conference
New York City, USA, Aug 30-Sept 3, 2006

COMPUTERIZED DETECTION OF LUNG TUMORS IN PET/CT IMAGES

Iyad Jafar[1], Hao Ying[1,2], Anthony F. Shields[2,3], Otto Muzik[2,4]

[1]Department of Electrical and Computer Engineering, [2]Karmanos Cancer Institute
[3]Department of Medicine, [4]Department of Pediatrics, Wayne State University, Detroit, MI 48202, USA

***Abstract* - More and more hybrid PET/CT machines are being installed in medical centers across the country as combining Computer Tomography (CT) and Positron Emission Tomography (PET) provides powerful and unique means in tumor diagnosis. Visual inspection of the images is a tedious and error-prone task and in many clinics the attenuation-uncorrected PET images are not examined by the physician, potentially missing an important source of information, especially for subtle tumors. We are developing a computer aided diagnosis software prototype that simultaneously processes the CT, attenuation-corrected PET, and attenuation-uncorrected PET volumes to detect tumors in the lungs. The system applies optimal thresholding and multiple gray-level thresholding with volume criterion to extract the lungs and to detect tumor candidates, respectively. A fuzzy logic based approach is used to reduce false-positive tumors. The remaining set of tumor candidates are ranked according to their likelihood of being actual tumors. We show the preliminary results of a retrospective evaluation of clinical PET/CT images.**

1. INTRODUCTION

Cancer is one of the most deadly diseases in the world, especially in the developing industrial countries. Medical imaging modalities such as CT, PET, SPECT, and MRI are commonly used as fundamental components for tumor detection. Because each of these modalities contains either structural data as in the case of CT and MRI, or functional data for the case of PET and SPECT, it is sometimes difficult to make accurate evaluation of suspicious tumor structures utilizing one single modality. Thus, it is clinically conventional now to combine data contained in structural and functional scans to more accurately pinpoint any abnormality in the body. For example, CT and PET are now being used for such purposes [1], especially after the emergence of the hybrid PET/CT scanners which eliminate the need for post-processing to align and coregister the volumes [2]; serious challenging tasks associated with the use of multi-modal imaging before the scanners were combined.

PET/CT scanners generate three different sets of image volumes that correspond to the CT, attenuation-corrected PET (AC-PET) and attenuation-uncorrected PET (AU-PET) volumes. The AC-PET volume is the result of the attenuation correction process that is applied to the AU-PET volume to account for attenuation, scattered photons, random coincidences, and differing sensitivities of individual image planes. Intrinsically, AU-PET volume contains areas of variable activity resulting from differences in photon absorption. For example, the skin generally shows high activity relative to deeper structures on the AU-PET. For this reason physicians usually consider the CT and the AC-PET volumes only for time-efficient examinations. However, this could potentially incur a loss of information due to the imperfection in the attenuation correction process which may result in eliminating some tumors and/or introducing artifacts that look like tumors in the AC-PET volume [3]. Even with just two volumes, visual examination with the naked eye could be a tedious and error-prone process due to the massive number of slices that each volume contains. One can imagine the required additional effort if the AU-PET volume is also examined. This motivates the need for a computer aided diagnosis (CAD) system that comprehensively utilizes the CT, AC-PET, and AU-PET volumes to assist physicians in their diagnosis by automatically detecting all possible tumors. In this paper we present a novel CAD system for tumor detection applied to images produced by the hybrid PET/CT scanners. The core of the system collectively utilizes the available three volumes in the PET/CT scans. This methodology strengthens the detection accuracy and reliability as takes advantage of the high-resolution structural information available in the CT and the metabolic functional information available in the AC-PET. In the meanwhile this approach reduces the detection error incurred by the attenuation correction process in the PET by the inclusion of the AU-PET volume in the processing.

The system carries out this task by employing different image processing techniques in both the 2D and 3D spaces. The entire process is summarized as follows. The region of interest (ROI) is segmented out from the CT volume using optimal thresholding and image morphing. The extracted ROI is then mapped to the spatially coregistered PET volumes. The ROIs from the three volumes are passed to a multiple-thresholding algorithm with volume criterion to independently detect all suspicious tumors in the three volumes. After the initial detection, a reduction process that is based on fuzzy clustering and fuzzy inference is applied to reduce false positive tumor candidates. To accommodate for the variations in the characteristics of the detected tumors and for the different clinical interpretations of each type of the PET/CT volumes, we use seven rules that are based on clinical experience to rank the tumors according to their likelihood of being tumors.

Generally, the proposed CAD system can be applied to any part in the body. However, we focus on the detection of lung tumors due to its significance. Several CAD systems have been proposed to detect lung tumors in CT such as

[4,5] and PET [3,6] *separately*. To the best of our knowledge, our system is the first system to computerize the detection of tumors using PET and CT images *jointly*.

2. ROI EXTRACTION AND TUMOR DETECTION

2.1 Extraction of the regions of interest

To extract the lungs out of the whole-body PET/CT scans, we utilize the iterative optimal thresholding algorithm [7] to calculate a threshold value L_{opt} that divides the image volume voxels into two clusters: ROI and background. For accurate ROI segmentation, thresholding uses the high contrast CT volume, since it is easier to distinguish the lungs from the remaining body structures in its histogram [4]. Applying the threshold value L_{opt} to the 3D volume produces an initial segmentation shown in figure 1.1-b. This initial result is imperfect because it considers the exterior of the body as part of the ROI and in the same time excludes parts of the ROI (the black islands within the lungs). To eliminate the structures that are exterior to the lungs, 3D sequential labeling with 26-neighbor connectivity is used to identify the largest two connected structures that don't touch the borders of the volume. The identified structures resemble the two lungs, which are then processed by adding to them a negative self-copy to their binary equivalent images then applying image closing morphology with a mask size of 5x5 to fill the excluded small islands and to fuse the breaks in the borders, respectively. As shown in figures 1-e and 1-f, the extracted ROI from the CT is finally mapped to the AC-PET and AU-PET volumes by selecting the corresponding voxels, since all three volumes have isotropic spatial characteristics after resampling and scaling the PET volumes.

2.2 Tumor detection and false-positive reduction

Lung tumors in both CT and PET volumes are typically characterized with higher intensities compared to their background. Hence, the detection algorithm applies multiple thresholding procedure with volume criterion to detect the tumors in each of the three PET/CT volumes. In this procedure, the volume under consideration is thresholded at equally spaced gray levels; starting from the double-mean value – the mean of voxels having intensities greater than the global mean of the lungs - and ending at the highest intensity level in the volume. At each of these threshold levels, sequential labeling is used to label 3D connected structures. After that, the volume of the labeled structures is checked such that those with volume falling in a pre-specified range are preserved as tumors candidates while larger or smaller ones are discarded. In our implementation, we set the separation between the threshold levels to 3 experimentally. The upper and lower volume bounds for acceptable tumors are set to 3 cm and 5 mm, respectively. The upper bound specification is based on the clinical definition of tumors [8] while the lower bound is specified experimentally to eliminate noisy structures.

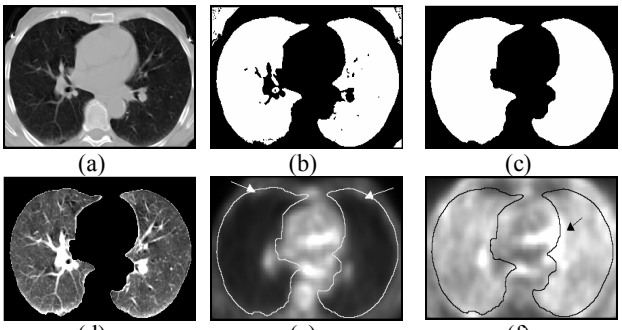

Fig.1. ROI segmentation steps: (a) source CT image, (b) initial thresholding of (a), (c) after closing, filling and background removal, (d) final segmentation, (e) and (f) mapping of lungs field to corrected and uncorrected PET

The application of the multiple thresholding procedure on the three PET/CT volumes results in a large number of tumor candidates, many of which are false positives and have to be removed. The presence of the airways and the pulmonary veins and arteries are the main sources of false positives in the CT volume. In the PET volumes, the scan process is conducted with the patient breathing and this causes the imaged lungs to be the averaged size of the lungs. Thus, when the ROI extracted from the CT is mapped to the PET volumes, part of the exterior of lungs is unintentionally included within the desired ROI as pointed by the arrows in Figures 1-f and 1-e. These external regions are of high intensity and are explicit sources of false tumors. To reduce these false-positive tumors extracted from the CT, AC-PET and AU-PET volumes, we use three Mamdani fuzzy inference systems [9] with singleton output fuzzy sets; one for each volume type. The motivation behind designing a separate fuzzy inference system for each of the PET-CT volumes is to accommodate for the variations and different interpretations of data between the volumes. However, the test for a new tumor, regardless of its source volume, invokes the use of the three systems to make use of the power of combining anatomical and structural imaging. Technically, to implement these systems, we first define their input feature space such that it is composed of three variables: tumor's contrast (COT), tumor's mean gray-level intensity (INT), and tumor's mean standard uptake value (SUV). The third variable, SUV, is a widely used measure for quantifying the uptake of ^{18}F-fluorodeoxyglocouse (^{18}F-FDG) in tumors based on the amount of injected tracer dose and patient's weight [10]. The SUV value for a specific region is defined as

$$SUV = \frac{ROI\ \ Activity\ \ Concentration\ \ [kBq/g]}{Injected\ Activity\ [kBq]\ /\ Body\ \ Weight\ [g]} \quad (1).$$

This SUV measure is calculated from the AC-PET volume only. So, to get SUV values for tumors in the CT and the PET-AU volumes, the activity of the corresponding location in the AC-PET volume is used. In the second step of the design, the domain for each of the input variables is partitioned to have two fuzzy sets, *High* and *Low*, with open-right and open-left trapezoidal membership functions, respectively, and as shown in figure 2. As the names imply, the *High* fuzzy set covers the upper portion of the domain, while the *Low* fuzzy set covers the lower portion.

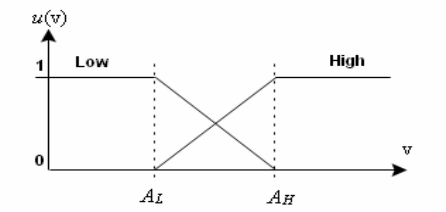

Fig. 2: Fuzzy sets used for input variables COT, INT, and SUV

To define the parameters A_L and A_H of the membership functions of these fuzzy sets, $\mu_v^{Low}(v)$ and $\mu_v^{High}(v)$, for each input variable v, we apply the unsupervised fuzzy clustering algorithm [11] on the features values extracted from a training set of tumors for each type of PET/CT volumes. In our implementation, this clustering algorithm is set up such that the training tumors samples in the 3D feature space are divided into two clusters: low-likelihood and high-likelihood. The centers of these clusters; (SUV_{LOW} ,INT_{LOW},COT_{LOW}) and (SUV_{HIGH},INT_{HIGH},COT_{HIGH}) are then used to assign numerical values for A_L and A_H . For instance, the A_L and A_H values for the contrast variable are assigned to COT_{LOW} and COT_{HIGH}, respectively. The last stage in designing the fuzzy inference systems is to define the *if-then*. In each of the three fuzzy inference systems, we define eight rules such that we cover all possible combinations of input fuzzy sets (2^3=8). The consequence part $\mu_i(y)$ of the ith rule is a singleton fuzzy set, which a set that has unity membership at a single point Y_i and zero elsewhere. For the ith rule, this can be defined mathematically at point Y_i by the Dirac-delta function as

$$\mu_i(y) = \delta(y - Y_i) \quad (2).$$

The value Y_i for the ith rule is assigned intuitively based on the clinical significance of the rule's condition. Table 1 lists these rules in ascending order depending on their diagnostic relevance.

If SUV **is** *Low* **&** INT **is** *Low* **&** COT **is** *Low*	**Then** $Y_1 = \delta(y\text{-}1)$
If SUV **is** *Low* **&** INT **is** *Low* **&** COT **is** *High*	**Then** $Y_2 = \delta(y\text{-}2)$
If SUV **is** *Low* **&** INT **is** *High* **&** COT **is** *Low*	**Then** $Y_3 = \delta(y\text{-}3)$
If SUV **is** *Low* **&** INT **is** *High* **&** COT **is** *High*	**Then** $Y_4 = \delta(y\text{-}4)$
If SUV **is** *High* **&** INT **is** *Low* **&** COT **is** *Low*	**Then** $Y_5 = \delta(y\text{-}5)$
If SUV **is** *High* **&** INT **is** *Low* **&** COT **is** *High*	**Then** $Y_6 = \delta(y\text{-}6)$
If SUV **is** *High* **&** INT **is** *High* **&** COT **is** *Low*	**Then** $Y_7 = \delta(y\text{-}7)$
If SUV **is** *High* **&** INT **is** *High* **&** COT **is** *High*	**Then** $Y_8 = \delta(y\text{-}8)$

Table 1: Fuzzy-if-then rules

Based on the definition of the three fuzzy inference systems, the decision of discarding a tumor candidate detected in any of the three PET/CT volumes is performed in three steps. First, the contrast (COT) and the intensity (INT) of the test tumor are calculated from the volume that this tumor belongs to, while the SUV is calculated always from the AC-PET volume. At the same time, the contrast and the intensity of corresponding locations of the tumor in the other two volumes are calculated. This calculation results in three triplets of values for the three features: (COT_{CT},INT_{CT},$SUV_{AC\text{-}PET}$), ($COT_{AC\text{-}PET}$,$IN_{\text{-}AC\text{-}PET}$,$SUV_{AC\text{-}PET}$) and ($COT_{AU\text{-}PET}$,$INT_{AU\text{-}PET}$,$SUV_{AC\text{-}PET}$). In the second step, each triplet is presented to the fuzzy inference system of the corresponding volume type such that the response/score of each system to the input triplet is calculated utilizing fuzzy inference [9]. Technically, three computational steps are invoked in fuzzy rule-based inference to calculate the output in any system X of the three fuzzy inference systems. These are:

1) Calculation of the degree of match DMi between the feature values of the tumor and the condition part of each the input rules. For instance the degree of match for rule 3 is given by

$$DM_3 = min(\mu_{SUV\_X}^{Low}, \mu_{INT\_X}^{High}, \mu_{COT\_X}^{Low}) \quad (3)$$

, where $\mu_{SUV\_X}^{Low}$, $\mu_{INT\_X}^{High}$, and $\mu_{COT\_X}^{Low}$ are the membership grades that of the input values SUV_X, INT_X, and COT_X , respectively.

2) Calculation of the output or score of each individual rule by scaling the output singleton with the degree of match

$$SCORE_i^X = DM_i \times \delta(y - Y_i) \quad (4)$$

3) Aggregation of the individual rules' scores into one score that represent the system response to the input. This is calculated using the weighted average formula given by

$$SCORE^X = \sum_{i=1}^{8} SCORE_i^X / \sum_{i=1}^{8} DM_i^X \quad (5)$$

After calculating the tumor scores in the three fuzzy inference systems, the third step calculates the average of these scores and compares it to an experimental threshold value of 6.5 (this corresponds to eliminating those candidate that don't meet 81% of the maximum score that any tumor can take, i.e. 8.0). If the tumor average score does not exceed this value, then it is discarded.

2.3 Tumors ranking

Applying the multi-thresholding algorithm on the three volumes to detect tumors does not guarantee that a specific tumor will show up in all the three volumes due to the difference in the intensity distribution and representation between the three volumes. In addition, tumors usually have different mean intensity and contrast depending on their likelihood of being tumors. Putting these together suggests the introduction of a ranking system where tumor candidates are ranked according to their likelihood of being tumors. In our system, we used four features to calculate the rank of the tumors: (1) *tumor concurrence* - whether the tumor or part of it occurs at the same location in more than one volume, (2) *tumor volume,* (3) *tumor intensity*, and (4) *tumor contrast.* After the calculation of these features for each tumor candidate, we use seven rules that are based on clinical experience to rank the tumor candidates as follows.

Rule 1: A tumor or part of it, occurring in the CT, the AC-PET and the AU-PET volumes is assigned the highest score to be true tumor.

Rule 2: A tumor, or part of it, occurring in the CT and the AC-PET volume is assigned the second highest score.

Rule 3: A tumor, or part of it, occurring in the CT and the AU- PET volume is assigned the third highest score.

Rule 4: A tumor, or part of it, occurring in the AC-PET and the AU-PET volumes is assigned the fourth highest score.

Rule 5: Remaining non-concurrent tumors from the AC-PET volume are assigned fifth highest score with each being assigned a sub score that is directly proportional to their mean intensity.

Rule 6: Remaining non-concurrent tumors from the AU-PET volume are assigned the seventh highest score with each being assigned a sub score that is directly proportional to their mean contrast.

Rule 7: Remaining non-concurrent tumors from the CT volume are assigned the sixth highest score with each being assigned a sub score that is directly proportional to their mean intensity.

The volume of the tumors is used to break the ties between tumors with the same contrast or mean intensity, with preference to smaller tumors. After the rank calculation, and for better visual representation, the scores of the tumors are coded into colors such that the higher the rank of the tumor, the closer its color to white.

3. PRELIMINARY RESULTS

Data in this study included three PET/CT scans that were acquired using Siemens Biograph 2-slice PET/CT scanner which yields a CT image volume with a pixel size of 0.98 mm (512x512 matrix) with a 5.0 mm slice thickness. The corresponding PET images have a pixel size of 5.15 mm (128x128 matrix) with a slice thickness of 2.43 mm. The PET volumes were upsampled and scaled to meet the CT specifications. To test the system performance, we adopted a leave-one-out scheme such that one of the cases is left on the side for testing while the remaining cases are used to train the three fuzzy inference systems. On average, the systems achieved 96%, 98%, and 97% reduction in the initial number of false-positive tumors detected by the multiple-thresholding algorithm when applied to the CT, AC-PET, and AU-PET volumes, respectively. The remaining tumor candidates are ranked according to the rules explained in section 3. To ease the comparison between the clinical diagnosis results and the CAD results, we considered tumors satisfying the first four rules as true tumors reported by the CAD system. Adopting such criterion revealed a reasonable preliminary performance of the system an overall sensitivity of 75% and 100% specificity. Figure 3 shows a sample result for a tumor satisfying rule 1.

4. CONCLUSIONS

We are developing a novel computerized system to ease and aid physicians in detecting subtle lung tumors in the scans produced by hybrid PET/CT machines. Preliminary retrospective evaluation using clinical PET/CT images showed promising results.

ACKNOWLEDGMENT

This research was supported in part by a Wayne State University Research Enhancement Grant.

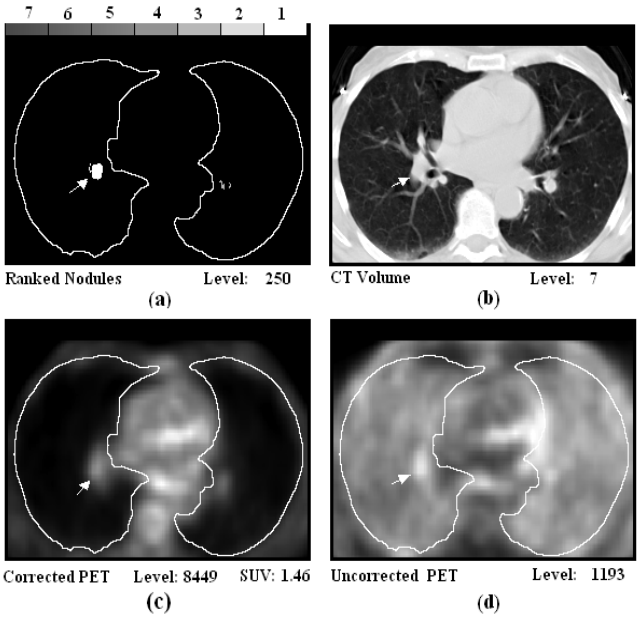

Fig.3. (a) tumor matching Rule 1 is marked and assigned the highest score. Corresponding locations as well as intensity and SUV values are shown in (b) CT (c) AC-PET and (d) AU-PET. The bar on the top of (a) shows the encoding of rule numbers into gray levels.

REFERENCES

[1] Janet Cochrane Miller, "PET/CT for Tumor Imaging," *Radiology Rounds*, Vol. 2, Issue 5, May 2004.

[2] David W. Townsend, Thomas Beyer, Todd M. Blodgett, "PET/CT Scanners: A Hardware Approach to Image Fusion", *Seminars in Nuclear Medicine*, Vol. XXXIII, No 3: pp 193-204, July, 2003.

[3] Hao Ying, Fule Zhou , Anthony Shields, Otto Muzik, Defang Wu, Elisabeth Heath, "A Novel Computerized Approach to Enhancing Lung Tumor Detection in Whole-Body PET Images," *Proceedings of the 26th Annual International Conference of the IEEE EMBS*, CA, USA, September 1-5, 2004.

[4] Binsheng Zhao, Gordon Gamsu, Michelle S. Ginsberg, Li Jiang, and Lawrence H. Schwartz, "Automatic Detection of Small Lung Nodules on CT Utilizing a Local Density Maximum Algorithm," JOURNAL OF APPLIED CLINICAL MEDICAL PHYSICS, VOLUME 4, NUMBER 3, SUMMER 2003.

[5] J. Ko, D. Naidich, " Computer-Aided Diagnosis and the Evaluation of Lung Disease," J Thorac Imaging • Volume 19, Number 3, July 2004.

[6] C. C. Huang, X. Yu and P. S. Conti, "Computer-aided lesion detection with statistical model-based features in PET images," *IEEE Trans. Nuclear Science*, vol. 44, no. 6, pp. 2509-2521, 1997.

[7] R. Gonzalez, R. Woods, "Digital Image Processing," 2nd edition, Addison-Wesley 1993.

[8] Tuddenham WJ. Glossary of terms for thoracic radiology: recommendations of the Nomenclature Committee of the Fleischner Society. AJR Am Roentgenol 1984; 143: 509-517.

[9] E. H. Mamdani, S. Assilian,"An Experiment in Linguistic Synthesis with a Fuzzy Logic controller," International Journal of Man-Machine Studies, 7(1):1-13,1975.

[10] Menda Y, Bushnell DL, Madsen MT, McLaughlin K, Khan D, and Kernstine KH, "Evaluation of various corrections to the standardized uptake value for diagnosis of pulmonary malignancy," *Nuclear Medicine Communications,* 22(10):1077-1081, October 2001.

[11] J. C. Bezdek, "Fuzzy Mathematics in Pattern Classification," PhD thesis, Applied Mathematics Center, Cornell University, Ithaca, 1973.